Reflective-Mode Phase-Variation Submersible Sensor for Liquid Characterization

Lijuan Su, *Member, IEEE*, Paris Vélez, *Senior Member, IEEE*, Pau Casacuberta, *Graduate Student Member, IEEE*, Jonathan Muñoz-Enano, *Member, IEEE*, Marta Gil-Barba, *Member, IEEE*, and Ferran Martín, *Fellow, IEEE*

***Abstract*— A one-port reflective-mode microwave submersible sensor based on an open-ended step-impedance microstrip line configuration, operating at a single frequency, useful for the dielectric characterization of liquids and for the measurement of liquid composition in binary mixtures, is proposed in this paper. The sensor constitutes two parts, namely, the microwave module, including the sensitive region, and a 3D-printed case (made of polylactic acid –PLA), necessary for sealing, thereby preventing from any liquid leakage to the non-sensing regions of the microwave module. To enhance the sensitivity, the open-ended line section of the microwave module, i.e., the sensing region in contact with the liquid under test (LUT), is a quarter-wavelength microstrip line with high impedance. Thus, the phase of the reflection coefficient is the output variable, highly dependent on the input variable –dielectric constant of the LUT placed directly above the sensing region. In order to validate the sensing structure, a prototype device has been designed and fabricated. The average sensitivity to variations in the concentration of ethanol in solutions of deionized (DI) water is 1.22º/%, and sensor resolution is 2%. The fabricated sensor is resistant to liquid leakage, and therefore it can be completely submersed for measuring purposes, acting as an effective measuring probe.**

***Index Terms*—absorption; dielectric characterization of liquids; microwave sensors; microstrip technology; permittivity measurement; phase-variation sensor; reflective-mode sensor; submersible sensor.**

I. Introduction

Recently, microwave sensors have attracted lot of attentions for applications such as dielectric characterization of materials including both solids and liquids, since they are very sensitive to the dielectric properties of the interacted materials [1]. Indeed, microwave sensors can be beneficial for the measurement of any physical, chemical, or biological variable related to (or with influence on) the permittivity. Examples include humidity sensors [2],[3], temperature sensors [4],[5], motion sensors [6]-[10], gas sensors [11],[12], biosensors [13]-[15], defect detectors [16],[17], etc. Microwave sensors are also of interest for acquiring material composition in homogenous substances since the relative concentration of different elements influences the complex permittivity of the composite. Particularly, microwave sensors have been employed to obtain the relative concentration of solute in binary [18]-[20] and ternary [21],[22] liquid mixtures.

For liquid characterization, most reported microwave sensors are based on microfluidic technology [13],[14],[18]-[20],[23]-[26], typically combined with planar sensing structures, e.g., implemented in microstrip or coplanar waveguide (CPW) technology. Typically, although not exclusively, in such sensors the fluidic channel is located on top of a sensing planar resonant element, such as a complementary split ring resonator (CSRR) [19], or a split ring resonator (SRR) [20],[23]. In microfluidic sensors, small amounts of liquids are needed, but the design and fabrication of such sensors is complicated. Moreover, careful and rigorous measurements should be carried out with microfluidic sensors, to prevent from the appearance of bubbles in the channel.

An alternative strategy for liquid sensing is the use of small containers (liquid pools or holders) [27],[28] which can be implemented, e.g., through 3D printing, and placed above the sensitive region of the sensor. In this case, small amounts of LUT typically suffice for measuring purposes, as well, and device fabrication is simple, as compared to microfluidics.

Finally, there are liquid sensors that act as a probe, as far as they can be submersed in the LUT. The most clear and well-known example is the so-called coaxial probe [29]-[35], commercially available [36]. The dielectric properties of the LUT can be obtained through coaxial probes with reasonably good accuracy. But the main disadvantage of the coaxial probe approach is related to the complex numerical techniques used to get the complex permittivity of the LUT from the measured reflection coefficient [typically collected through a vector

This work was supported in part by MCIN/AEI, Spain, through ERDF European Union under Grant 10.13039/501100011033 and Grant PID2019-103904RB-I00; in part by the European Union Next Generation EU/PRTR under Grant PDC2021-121085-I00 and Grant CPP2021-009080; in part by the AGAUR Research Agency, Catalonia Government, under Project 2021SGR-00192; and in part by Institució Catalana de Recerca i Estudis Avançats (who awarded Ferran Martín). The work of Lijuan Su was supported by the Juan de la Cierva Program under Project IJC2019-040786-I. The work of Pau Casacuberta was supported by the Ministerio de Universidades, Spain, through the FPU (Ayudas para la formación de profesorado Universitario) under Grant FPU20/05700. Marta Gil-Barba acknowledges the Multiannual Agreement between Polytechnic University of Madrid and Madrid Government for the support in the context of the V PRICIT (Regional Programme of Research and Technological Innovation) in the line Excellence Program for University Professoriate (Ref. M190020074B).

L. Su, P. Vélez, P. Casacuberta, J. Muñoz-Enano, and F. Martín are with CIMITEC, Departament d'Enginyeria Electrònica, Universitat Autònoma de Barcelona, 08193 Bellaterra, Spain. Email: Lijuan.Su@uab.cat.

M. Gil-Barba is with Departamento Ingeniería Audiovisual y Comunicaciones, Universidad Politécnica de Madrid, 28031 Madrid, Spain.

Color versions of one or more of the figures in this article are available online at http://ieeexplore.ieee.org.

network analyzer (VNA)], see [1] and references therein. Other submersible liquid sensors implemented in planar technology, operating either in transmission-mode [37],[38] or in reflection-mode [39],[40], have been recently reported. The transmission-mode sensors of [37] exploit the resonance frequency variation generated in a SRR due to the influence of the LUT. In the submersible sensors based on reflective-mode presented in [40], the sensing principle is also frequency variation, but the output variable in this case is the return loss.

One limitation of frequency-variation sensors, as those reported in [27],[28],[37],[40],[41]-[50], concerns the need to excite the sensor by a wideband sweeping interrogation signal, at least covering the output dynamic range. To alleviate such limitation, we propose a single-frequency sensor in this paper. There are mainly two kinds of single-frequency sensors, i.e., coupling modulation sensors [6],[7],[9],[51]-[56], mostly utilized to the measurement of motion variables, and phase-variation sensors [57]-[68], of special interest for permittivity characterization, and for the determination of related variables, e.g., liquid composition, the interest in this work. Thus, we present a reflective-mode microwave sensor based on phase variation that operates at a single frequency in this paper. The sensor is utilized for the determination of the composition of binary liquid composites, particularly mixtures of ethanol in DI water. The sensor topology is optimized to achieve the highest possible sensitivity (with reduced dimensions) in the range of the permittivity of DI water, provided the interest is the characterization of small concentrations of ethanol in DI water. It will be illustrated that the sensor is equipped with a 3D-printed polylactic acid (PLA) case to avoid liquid leakage to the non-sensitive regions of the sensor, thereby providing good sealing. Such sealing is necessary since the appearance of liquid outside the sensing region of the device might generate false readings.

The paper is structured as follows. The sensor concept, design, and fabrication process are presented in Section II. Section III is devoted to sensor validation, by considering simulations and measurements. The competitive advantages of the proposed sensor and comparison with other submersible sensors is the subject of Section IV. In Section V, high impedance contrast between the sensing line and the so-called design line for sensitivity enhancement is further theoretically explained, with a detailed elaboration on the analogy between the 90º open-ended sensing line and a series resonator. Emphasis is also put on the analysis of the effects of LUT losses, which turn out to be helpful for boosting up the sensitivity in the limit of small perturbations of the reference LUT. Finally, the main concluding remarks are highlighted in Section VI.

II. Sensor Concept, Design, and Fabrication

The proposed sensor constitutes two main parts, i.e., a microwave module and a sealing case (mechanical module). The microwave part is based on a step-impedance transmission line configuration first reported in [60], and such module is implemented in microstrip technology in this work. As it was presented in [60], highly sensitive one-port reflective-mode phase-variation sensors can be achieved by cascading a set of quarter-wavelength transmission line sections with high/low impedance to a sensing element (the one that should be in contact with the LUT) consisting of a planar resonator. Such sensing resonator can be a distributed resonator [60]-[62] or a semi-lumped (i.e., planar, and electrically small) resonator [67]-[68]. In this paper, the sensor is implemented by considering the former option, that is, a distributed resonator, particularly an open-ended quarter-wavelength resonator with high-impedance. In order to boost up the sensitivity, the quality factor of the resonator should be high. For this main reason, the characteristic impedance of the open-ended quarter-wavelength transmission line sensing resonator should be set to a high value (as compared to the reference impedance of the port, typically $Z_0 = 50\ \Omega$).

Figure 1 depicts a sketch (layout) of the sensor configuration (microwave module), where the sensor consists of the open-ended (quarter-wavelength) transmission line sensing resonator and a single quarter-wavelength line section (designated as design line) cascaded to it, plus the access line (which should be matched to the port, and consequently exhibiting a characteristic impedance of $Z_0 = 50\ \Omega$). Note that the design line should exhibit a low characteristic impedance, *Z*. This impedance contrast is necessary to enhance the sensitivity in the limit of small perturbations, i.e., for small changes in the permittivity of the LUT close to the reference (REF) value (DI water in our case), as indicated in [60]. The sensitivity in that limit is given by [60]

$$S = -\frac{Z_s Z_0 (1-F)}{2Z^2 \varepsilon_{\text{eff}}}\phi_s = -\frac{\overline{Z_s}}{\bar{Z}^2}\frac{(1-F)}{2\varepsilon_{\text{eff}}}\phi_s \qquad (1)$$

where Z_s is the characteristic impedance of the sensing line and ε_{eff} is the effective dielectric constant of the sensing line when it is loaded with the REF liquid (DI water), i.e.,

$$\varepsilon_{\text{eff}} = \frac{\varepsilon_r + \varepsilon_{\text{REF}}}{2} + \frac{\varepsilon_r - \varepsilon_{\text{REF}}}{2}F \qquad (2)$$

ε_r being the substrate dielectric constant, ε_{REF} the dielectric constant of the REF liquid, and *F* a geometry factor that depends on the width of the microstrip line, w_s, and thickness of the substrate, *h*, according to

$$F = \left(1 + 12\frac{h}{w_s}\right)^{-1/2} \qquad (3a)$$

provided $w_s > h$. If $w_s < h$, the geometry factor is

$$F = \left(1 + 12\frac{h}{w_s}\right)^{-1/2} + 0.04\left(1 - \frac{w_s}{h}\right)^2 \qquad (3b)$$

In (1), $\phi_s = 90^\text{o}$ is the electrical length of the sensing line loaded with REF liquid at the operating frequency. Note also that the normalized impedance values $\overline{Z_s} = Z_s/Z_0$ and $\bar{Z} = Z/Z_0$ have been used in (1). The validity of (3) requires that $t << h$, as usually satisfied, where *t* is the thickness of the metallic layer. Note also that expression (2) is valid provided the LUT is thick

enough to guarantee that the electric-field lines generated by the sensing line are completely circumscribed within the LUT, a reasonable approximation in a submersible sensor.

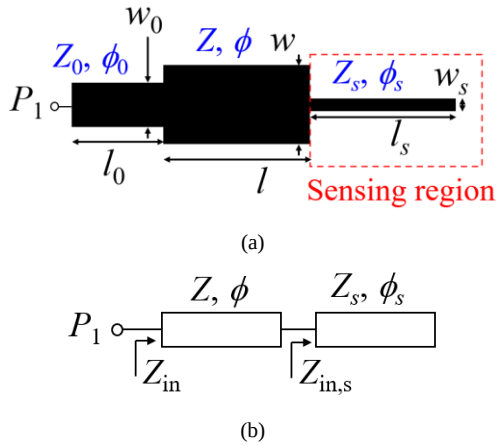

Fig. 1. Layout of the one-port reflective-mode phase-variation sensor based on a step-impedance microstrip line configuration consisting of an open-ended high-impedance quarter-wavelength sensing line cascaded to a low-impedance quarter-wavelength design line (a), and the schematic circuit (excluding the access line) (b). Dimensions (in mm) are: w_s = 0.2, l_s = 24.15, w = 7.5, l = 38.06, w_0 = 3.36, l_0 = 15. Note that these line dimensions, providing the impedances and electrical lengths indicated in the text, are under the condition that a narrow PET film (with thickness of 0.06 mm), used to avoid substrate absorption, covers the design line and sensing line sections.

In order to avoid that the non-sensitive parts of the microwave module (i.e., the design line) are in contact with the LUT when the sensor is submersed, a sealing case (mechanical part) is necessary. It should be windowed, so that the sensitive region can be in contact with the LUT. The proposed solution uses two covers made of polylactic acid (PLA) by means of 3D printing. In the bottom cover, the shape of the substrate that supports the microwave module is molded, so that it can be adapted to the bottom cover. The upper cover has a uniform thickness, but it contains a window around the sensitive region. The sketch of the covers is shown in Fig. 2. According to these comments, it is clear that the design line is coated with PLA, but not the sensing line, covered with the LUT when the sensor is submersed. Actually, a film of PET coats the whole microwave module, except the access line, preventing from the problem of substrate absorption. The presence of this PET film degrades the sensitivity, as it will be later shown. Nevertheless, this loss of sensitivity can be compensated by cascading further high/low quarter-wavelength transmission line sections to the sensor if it was necessary. The different parts of the sensor are then assembled with silicone rubber compound, and liquid leakage to the non-sensitive parts of the microwave module is thus prevented.

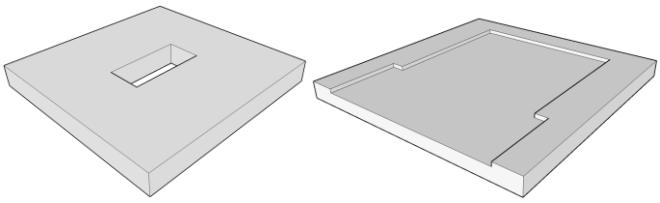

Fig. 2. Sketch of the case. Top cover (a) and bottom cover (b).

As mentioned previously, the design line and the sensing line are both coated with PET. In order to obtain an optimized sensitivity, the electrical length of the design line should be ϕ = 90º when it is covered with PET film (with dielectric constant of 3, and thickness of 0.06 mm) and PLA (with estimated dielectric constant of 2.8, and thickness of 8 mm to guarantee that the electromagnetic field lines do not cross the PLA/air interface). The electrical length of the sensing line should also be ϕ_s = 90º, as indicated, when it is coated with PET film and submersed in the REF liquid, DI water in this work, with dielectric constant of 80.86 at the operating frequency, set to f_0 = 1 GHz. Both electrical lengths must be satisfied at f_0. Note that the value of f_0 has been chosen as a tradeoff, i.e., at this frequency, sensor dimensions are reasonably small, whilst the measuring set-up is relatively simple (a moderately low frequency and low-cost vector network analyzer suffice). The dimensions of the different line sections when coated with the PET film, are included in the caption of Fig. 1.

Concerning the line impedances, the characteristic impedance of the PLA-coated quarter-wavelength (design) line is Z = 27.06 Ω, whereas the characteristic impedance of the sensing line has been set to Z_s = 75.11 Ω (with the presence of REF liquid and PET film). Figure 3 depicts the perspective view and photograph of the whole fabricated sensor, as well as the microwave module. The microwave part has been fabricated on the *Rogers RO4003C* substrate, with dielectric constant ε_r = 3.55, loss tangent tanδ = 0.0022, and thickness h = 1.524 mm, through a drilling machine (*LPKF H100*). The case has been fabricated using the 3D printer *Ultimaker 3 extended* model.

To end this section, let us mention that it has been verified by electromagnetic simulation (not shown) that the fringe fields in the quarter-wavelength sensing line do not extend beyond the window corresponding to the PLA case and are therefore circumscribed within the liquid under test (provided the sensor is submersed in it). Therefore, these fringe fields do not affect the accuracy of the sensor.

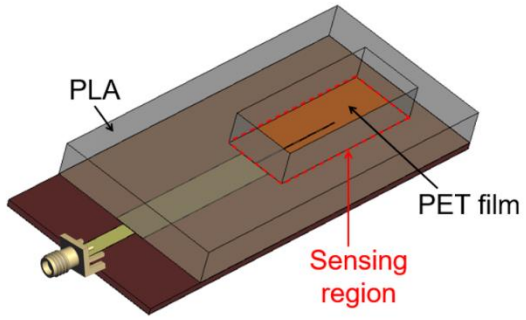

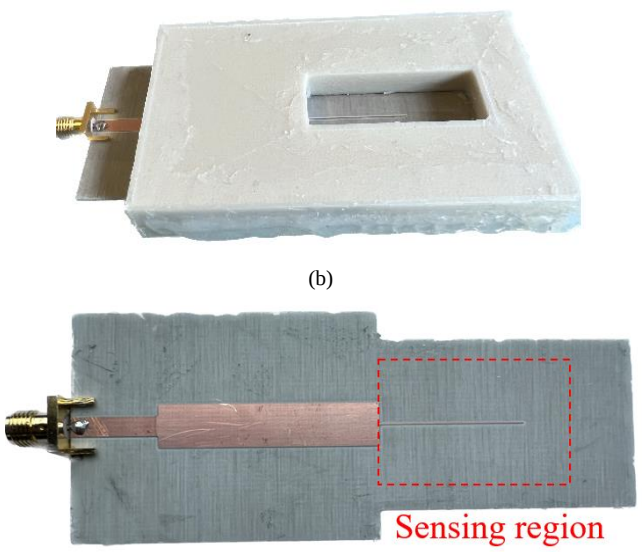

(b)

(c)

Fig. 3. Perspective view (a) and photograph (b) of the fabricated submersible sensor, and top-view photograph of the microwave module (c). The perspective view indicates the PET film in orange, the PLA top cover in grey, and the sensing region in red dash lines. Dimensions are indicated in the caption of Fig. 1.

III. Validation

For sensor validation, the fabricated sensor has been submersed into a glass beaker filled with DI water mixed with different proportions of ethanol, as shown in Fig. 4. Before experimental validation, the phase of the reflection coefficient of the proposed bare sensor (i.e., without any LUT loaded in the sensing region), and for the sensor covered with DI water (with dielectric constant 80.86 at 1 GHz), has been inferred by full-wave simulation, using the *CST Microwave Studio* commercial software. Figure 5(a) depicts these simulated phase responses. Such figure also contains the measured phase responses, obtained by VNA *Keysight N5221A*. One-port calibration of the VNA *Keysight 5221A* has been performed using a *Keysight N7554A* electronic calibration module. Power of the source of the VNA was set as default (0 dBm). Port extension has been done using open-short-load stubs to make the reference plane of the measurements at the input port. For the measured response with DI water, the fabricated sensor has been submersed to the glass beaker full of DI water. An excellent agreement between the electromagnetic simulations and measurements can be appreciated in Fig. 5(a). We have also performed measurements for different mixtures of pure ethanol and DI water. The corresponding phase responses are illustrated in Fig. 5(b). It can be appreciated that the phase at the operating frequency goes through a significant change as the percentage of ethanol in the mixtures varies.

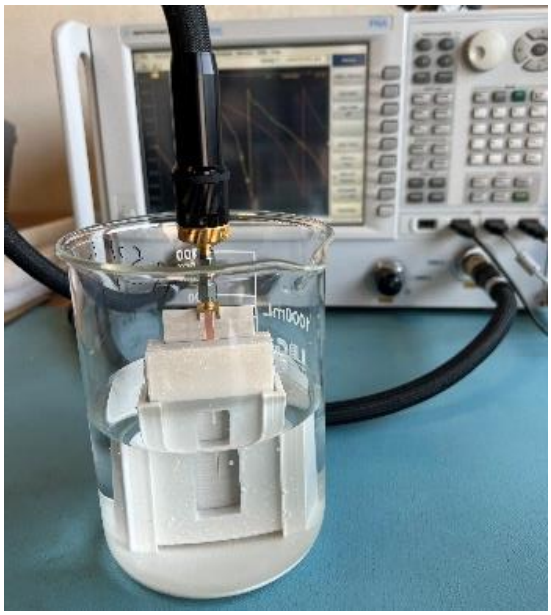

Fig. 4. Measurement setup.

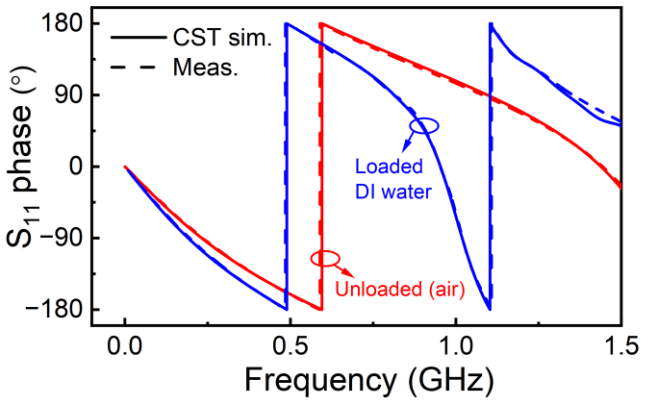

(a)

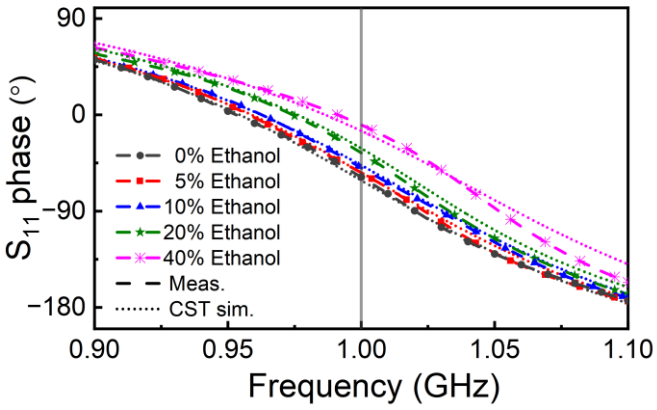

(b)

Fig. 5. Measured and simulated phase response of the proposed sensor when it is unloaded (bare sensor) and loaded with the REF liquid –pure DI water (a), and simulated and measured phase responses in the frequency region around the operating frequency, corresponding to the fabricated sensor submersed in LUTs of different proportions of ethanol in DI water (b). In the simulated responses in the *CST Microwave Studio* commercial software, the dispersive Debye model of DI water is used, while for the different mixtures, the dielectric

parameters (including losses) are obtained from the average of Weiner model. Note that in all the phase responses (simulated and measured), the effects of the access line are included. The measurements have been carried out at ambient temperature (23ºC).

The electromagnetic simulations for various mixtures of ethanol and DI water have also been performed by setting the dielectric constant of the LUT to different values between the dielectric constant of pure ethanol (27.86 at 1 GHz) and that of pure DI water (80.86 at 1 GHz). In order to estimate the agreement between the simulated results and the measured ones, and calculate the sensitivity, the dielectric constant for various considered ethanol concentrations has been obtained. For that purpose, we have used the *Keysight ADS* co-simulation to tune the dielectric constant of the mixture until the phase response matches the measured one. To be more specific, let us consider, for example, that the fabricated sensor is submersed in a mixture consisting of 95% DI water and 5% of ethanol, and that the phase response is obtained (measured) with the VNA. Then, in *Keysight ADS* co-simulation, we tune the dielectric constant of the mixture until the phase response from the *ADS simulator* matches the measured phase. A dielectric constant value, 77.5, is obtained for the LUT from this procedure, which corresponds to the permittivity of the considered mixture (5% of ethanol in DI water). Using the same procedure, the dielectric constant for other concentrations of ethanol in DI water has also been obtained. Figure 6(a) demonstrates that the dielectric constants of the different LUTs (corresponding to different concentration of ethanol in DI water), inferred by the indicated procedure, are circumscribed within the Weiner model limits [69], and has good agreement with the average dielectric constant of mixtures estimated from Weiner model [depicted in blue curve in Fig. 6(a)]. Thus, the way for retrieving the dielectric constant of the LUT is validated. Figure 6(b) illustrates the variation of the measured and simulated (using *CST Microwave Studio* commercial software and setting the dielectric constant of mixtures as the values obtained in the previous procedure) phase of the reflection coefficient at the operating frequency, f_0, as a function of the dielectric constant of different mixtures of ethanol and DI water. As it can be appreciated, there is good agreement between measured and simulated phase variations.

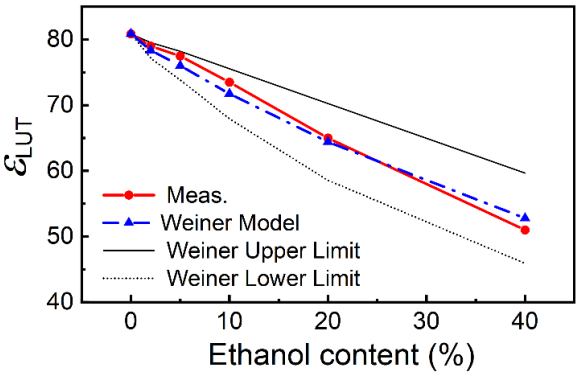

(a)

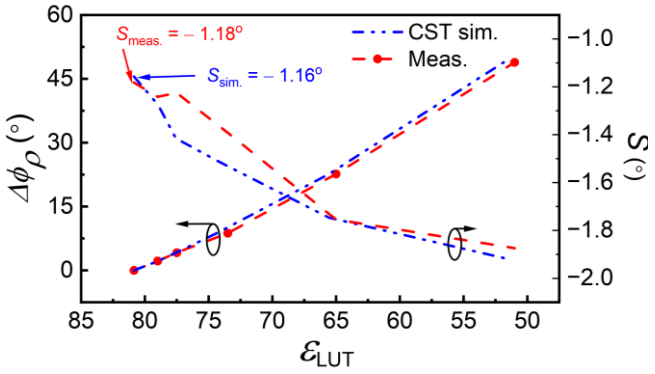

(b)

Fig. 6. Dielectric constant as a function of the percentage of ethanol in DI water, and indication of the upper/lower and averaged values as dictated by the Weiner model (a). Variation of the phase of the reflection coefficient at f_0 with the dielectric constant of the mixture, inferred from measurement and *CST Microwave Studio* commercial software, and the sensitivity (b). Note that for the phase variation and sensitivity in *CST* simulation, the dielectric constant of mixtures is from Fig. 6(a) of measured results, and the loss tangent of mixtures is from the average loss tangent of Weiner model. The measurements have been carried out at ambient temperature (23ºC).

The sensitivity of the sensor is also included in Fig. 6(b), as inferred by numerically obtaining the derivative of the phase with the dielectric constant of the LUT, ε_{LUT}, for both the measured and simulated data points. The small discrepancies are attributed to the fact that small differences between the measured and simulated values of the phase generate non negligible (though small) discrepancies in the derivative. The differences between the simulated and measured phases are caused by several reasons, including the possible presence of bubbles, fabrication-related tolerances, and the encapsulation of the top and the bottom PLA covers (with some silicone rubber compound applied to the design line region). Potential causes of error in the measured phase may be originated by the coaxial cable, temperature variations, unproper positioning of the submersible sensor, or even thermal drifts in the VNA. Nevertheless, it should be mentioned, as it can be appreciated in Fig. 6(b), that the output variable, the phase of the reflection coefficient, is referred to the phase when the sensor is submersed in the reference liquid (pure DI water in this work). This helps in improving the accuracy. Also, it should be mentioned that the temperature has been set to roughly 23ºC to minimize the impact of it in the measurements.

The sensitivity in the limit of small perturbations (i.e., around the dielectric constant of the REF LUT, i.e., DI water) is very similar for measurement and simulation. It should be mentioned that these sensitivity values, shown in Fig. 6(b), do not match with the theoretical prediction, provided by expression (1), since the use of the PET film for prevention of substrate absorption in the sensing region makes the equation invalid. Namely, despite the fact that the PET film has a thickness of 0.06 mm, many field lines are concentrated in such film, and the sensitivity is not correctly given by expression (1), in which it has been assumed that a semi-infinite LUT (without any protective film) covers the sensing region. The main reason why expression (1) is not valid when a PET film is coated

between the sensing line and the LUT is as follows. The sensitivity can be expressed as

$$S = \frac{d\phi_\rho}{d\varepsilon_{\mathrm{LUT}}} = \frac{d\phi_\rho}{d\phi_s}\frac{d\phi_s}{d\varepsilon_{\mathrm{eff}}}\frac{d\varepsilon_{\mathrm{eff}}}{d\varepsilon_{\mathrm{LUT}}} \quad (4)$$

since the contribution related to the effects of a variation of $\varepsilon_{\mathrm{LUT}}$ on ϕ_ρ through the variation of the characteristic impedance of the sensing line are null when the electrical length of the line is 90º, as demonstrated in [60]. The terms $d\phi_\rho/d\phi_s$ and $d\phi_s/d\varepsilon_{\mathrm{eff}}$ in (4) do not depend on the characteristics of the LUT, contrary to the last term, which cannot be inferred from expression (2) if the PET film is present. Thus, by assuming an unknown analytical dependence of $\varepsilon_{\mathrm{eff}}$ on $\varepsilon_{\mathrm{LUT}}$, the sensitivity in the limit of small perturbations can be expressed as

$$S = -\frac{Z_s Z_0 \phi_s}{Z^2 \varepsilon_{\mathrm{eff}}}\frac{d\varepsilon_{\mathrm{eff}}}{d\varepsilon_{\mathrm{LUT}}} \quad (5)$$

and the sensitivity when the PET film is present can be calculated, provided the characteristic impedances, the effective permittivity, and the derivative of effective permittivity with the dielectric constant of LUT are known. We have thus calculated the effective permittivity, the characteristic impedance, as well as the derivative of the effective permittivity with the dielectric constant of the LUT through the *ANSYS HFSS* commercial software. Such software directly provides the variation of the characteristic impedance and effective dielectric constant of the sensing line as a function of $\varepsilon_{\mathrm{LUT}}$, and, from the latter, the derivative $d\varepsilon_{\mathrm{eff}}/d\varepsilon_{\mathrm{LUT}}$ can be easily obtained. Thus, Z_s, $\varepsilon_{\mathrm{eff}}$, and $d\varepsilon_{\mathrm{eff}}/d\varepsilon_{\mathrm{LUT}}$ for $\varepsilon_{\mathrm{LUT}} = \varepsilon_{\mathrm{REF}}$ can be evaluated. Introducing in (5) these values, we have been able to calculate the sensitivity in the limit of small perturbations, and the sensitivity has been obtained to be $S_{\mathrm{th}} = -1.09º$. This theoretical sensitivity coincides with the values deduced from the simulated and measured results, indicated in Fig. 6(b), to a good estimation. Nevertheless, by including the effects of losses in the sensitivity analysis (to be discussed in Section V), the predicted sensitivity in the limit of small perturbations is somehow closer to the simulated (by including losses) and measured value, as it will be latter shown.

As compared with the sensitivities achieved in other reflective mode phase-variation sensors [60],[67],[68], the achieved sensitivity in the designed and fabricated sensor is moderated due to two main reasons. On one hand, the REF material is DI water with very high dielectric constant. Such high dielectric constant of the REF material reduces the sensitivity in the limit of small perturbations, since it determines the effective dielectric constant (also high) that appears in the denominator of (5). On the other hand, the use of the PET film significantly degrades the sensitivity, since many field lines generated by the sensing line are contained in such film. Nevertheless, the sensitivity can be improved, if necessary, by cascading further quarter-wavelength design line sections. For comparison purposes, Table I illustrates the relevant parameters of the proposed sensor and the sensitivity in the limit of small perturbations, by considering four cases, particularly, the sensor coated with PET film, unloaded and loaded with DI water, and the sensor not coated with PET film, also unloaded and loaded DI water. This table corroborates that the sensitivity in the limit of small perturbations dramatically decreases when the REF sample is DI water. The effects of the PET film are also significant, especially when the REF material is DI water, since the relative variation of the sensitivity is much higher in that case (from −5.53º to −1.09º). Note that the sensitivities when the REF is air are much higher (−167.0º without PET film, and −118.4º with PET film).

TABLE I: RELEVANT SENSOR PARAMETERS AND SENSITIVITY IN THE LIMIT OF SMALL PERTURBATIONS FOR THE CASES INDICATED IN THE TEXT

Case	Z_s (Ω)	$\varepsilon_{\mathrm{eff}}$	$d\varepsilon_{\mathrm{eff}}/d\varepsilon_{\mathrm{LUT}}$	l_s (mm)	Sensitivity (º)
Air/No PET	150.29	2.39	0.47	48.48	−167.0 from (1)
Air/PET	143.63	2.62	0.35	46.34	−118.4 from (5)
Wat./No PET	48.25	23.22	0.16	15.56	−5.53 from (1)
Wat./PET	75.11	9.58	0.02	24.15	−1.09 from (5)

Note that l_s is a quarter wavelength at the operating frequency.

As mentioned, the sensitivity in the proposed sensor can be increased by simply adding extra line sections with quarter wavelength. However, an increase in the sensitivity has the penalty of a degradation in the sensor linearity. The linearity in the proposed sensor is good, as Fig. 6(b) reveals, whilst the sensor can identify 2% ethanol concentration in DI water. This resolution is reasonable, but it could be increased by increasing the sensitivity by means of the indicated procedure. In summary, the reported submersible sensor has a reasonable sensitivity, resolution, and linearity combination, linearity being the sensor indicator with better performance. However, it is possible to optimize the sensitivity and resolution by sacrificing the linearity.

IV. COMPETITIVE ADVANTAGES, PROS, AND CONS

The proposed sensor can be used to characterize binary mixtures of liquids. For that purpose, it suffices to simply submersing the sensitive region into the LUT, similar to a measuring probe. To the best of authors' knowledge, the reported sensor is the first submersible sensor based on phase variation and operated in reflection at a single frequency. The achieved sensitivity is certainly moderate, but the main reason is the high dielectric constant of the REF liquid (DI water), as mentioned, not an improper sensor design. Other reported reflective-mode phase-variation sensors exhibit superior sensitivity [60],[67],[68], but in those sensors, the REF sample is either air, or a low dielectric constant material. In other words, the sensitivity of the phase-variation sensors reported in [60],[67],[68] would be comparable to the one of the sensors of Fig. 3, provided the considered REF material was DI water (or, alternatively, the sensitivity of the present sensor would be much higher by considering air as REF, as demonstrated in the previous section, see Table I).

A faithful comparison between a certain set of sensors necessarily should consider sensing devices dedicated to the measurement and characterization of the same type of materials

(high dielectric constant liquids in our case) and based on similar approaches and technologies. However, there are not reflective-mode phase-variation submersible liquid sensors in the available literature. Thus, a quantitative comparison of the sensor proposed in this paper with other reported submersible sensors is not representative, even by considering submersible sensors implemented in planar microwave technology, as those of refs. [37]-[40]. Nevertheless, a qualitative comparative analysis is possible.

The device reported in [37] is a transmission-mode submersible sensor consisting in a transmission line loaded with a pair of SRRs. That sensor was devoted to the characterization of oils (with a relatively small dielectric constant), and the sensing principle was frequency variation, obtained by the notch by changing the LUT where the sensor was submersed. The device presented in [38] is also a transmission-mode sensor based on a compact split ring resonator excited by two integrated monopole antennas, and the working principle of that sensor is also the variation of the notch frequency generated by changes in the dielectric constant of the LUT. The considered samples in [38] were acetone and different types of alcohols, in all cases with dielectric constants below 40. The sensitivities of these sensors are reasonably good. Specifically, in [37], a relative frequency shift of 22.04% for a variation of the dielectric constant of the LUT in the range between 2.45 and 22.52 was reported, whereas the relative frequency variation in [38] for a dielectric constant span from 20 to 40 was 23.52%. In the sensor of Fig. 3, the average sensitivity for dielectric constants varying in the range between 80.86 (pure DI water) and 51 (40% ethanol in DI water) is −1.6º (giving 1.22º/% in percentage of ethanol), sufficient to resolve variations of ethanol concentration of the order of 2%. Two advantages of the sensor of Fig. 3 over those of refs. [37], [38] are: (i) operation in reflective-mode, which requires one connector and reduces the length of the access line, as compared to the lengths of the access lines in the transmission-mode sensors of [37], [38]); (ii) operation at a single frequency, important to reduce the cost of the related electronics in operational environment (since a harmonic oscillator suffices to excite the sensor).

The submersible sensors reported in [39], [40] operate also in reflection mode, though their working principle is frequency variation, and, therefore, a sweeping interrogation signal covering the output dynamic range is required for sensing (in contrast to the sensor presented in this work). In these resonant sensors, the frequency of the notch in the reflection coefficient depends on the dielectric properties of the LUT and is thus the main output variable. The relative frequency shifts demonstrated in [39] and [40] are 36% (for dielectric constants changing in the range 25-55) and 1.3% (for dielectric constants changing in the range 7.60-7.54), respectively. These sensitivities, as well as those of the sensors reported in [37],[38], given in the preceding paragraph, are reasonably good (note that a comparison with the sensitivity of our sensor is meaningless since the output variables are different). However, it is not possible to enhance the sensitivity of the submersible sensors of [37-40] by adding microwave circuitry. By contrast, in the submersible sensors presented in this work, sensitivity can be boosted up, as mentioned, by adding additional quarter-wavelength line sections with high/low impedance. This is a unique and pertinent aspect of these reflective-mode phase-variation sensors.

Let us also mention that a novel aspect of the proposed sensor is the use of a sealing case, implemented by a 3D printer. Only the sensitive region is left to be in direct contact with the LUT. The case ensures that the design line section is not affected by the LUT, a necessary condition to avoid any phase perturbation caused by liquid leakage. The frequency-variation sensors proposed in [37]-[40] are more tolerant to the appearance of liquid outside the sensitive region (area occupied by the sensing resonators), since this does not significantly affect the notch frequency (of either the transmission or reflection coefficient). Nevertheless, in some of these sensors, the notch magnitude is also used as an additional output variable, and, in this case, the presence of LUT in the access line might vary the results, generating false readings. This aspect can be alleviated by carefully positioning the submersible sensor in the same location within the liquid under study, or, alternatively, by means of a sealing, case, the procedure considered in this work.

V. Discussion

Let us next elaborate on the ultimate reason explaining the need to implement the reported sensor with high impedance contrast between the sensing line and the design line, to enhance the sensitivity in the limit of small perturbations of the dielectric constant in the vicinity of the reference (REF) dielectric constant. The key aspect to achieve a high sensitivity in such limit is to achieve a high slope in the phase response of the reflection coefficient at the operating frequency. When the dielectric constant of the material under test (LUT in our case) varies, caused by a change in the relative concentration of ethanol, such variation either shifts up or down the phase response. Therefore, the excursion experienced by the phase of the reflection coefficient at the operating frequency increases with the phase slope, as illustrated in Fig. 7.

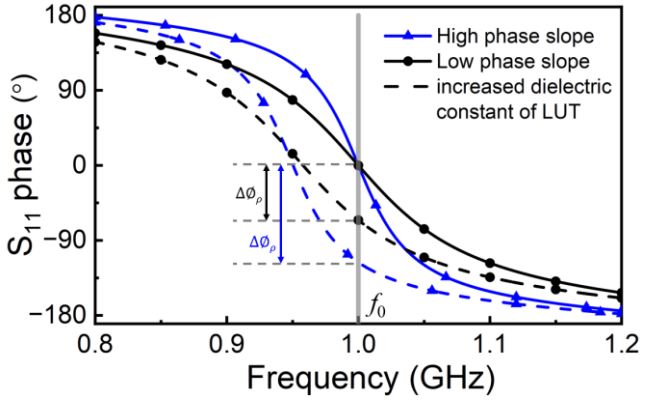

Fig. 7. Illustration of the phase excursion at a single frequency experienced by the reflective-mode phase-variation sensor in Fig. 1 when a change in the dielectric constant of the LUT occurs. Two cases are shown, i.e., with low and with high phase slope. Note that the change in the dielectric constant corresponds to 10% variation of the dielectric constant of the REF LUT.

It is well known that the slope in the phase of the reflection coefficient of a resonant element increases with the quality factor (*Q*-factor) [70]. For that main reason, a high characteristic impedance for the 90º open-ended sensing line (with a behavior similar to the one of a series resonator) is

required to boost up the sensitivity (corresponding to a high-*Q* resonator). To demonstrate that the 90º design line should exhibit a low characteristic impedance, let us infer the phase of the reflection coefficient. For that purpose, we must first express the impedance seen from the input port (excluding the access line) as a function of the electrical parameters of the structure [see Fig. 1(b)], i.e.,

$$Z_{\text{in}} = \frac{Z^2}{Z_{\text{in,s}}} \tag{6}$$

where it has been assumed that the 90º line behaves as an ideal impedance inverter (reasonable for frequencies in the vicinity of the operating frequency, the interest in this work). In (6), $Z_{\text{in,s}}$ is the impedance seen from the transverse plane between the design line and the sensing line, see Fig. 1(b), namely [70]:

$$Z_{\text{in,s}} = -jZ_s \cot \phi_s \tag{7}$$

where the effects of losses are excluded. The reflection coefficient is thus

$$\rho = \frac{Z_{in} - Z_0}{Z_{in} + Z_0} \tag{8}$$

Introducing (6) in (8), the following result is obtained:

$$\rho = \frac{\frac{Z^2}{Z_0} + jZ_s \cot \phi_s}{\frac{Z^2}{Z_0} - jZ_s \cot \phi_s} \tag{9}$$

The phase of the reflection coefficient is

$$\phi_\rho = 2\arctan\left(\frac{Z_0 Z_s \cot \phi_s}{Z^2}\right) \tag{10}$$

and the derivative with the angular frequency is found to be

$$\frac{d\phi_\rho}{d\omega} = \frac{d\phi_\rho}{d\phi_s}\frac{d\phi_s}{d\omega} = -\frac{2}{1+\left(\frac{Z_0 Z_s \cot \phi_s}{Z^2}\right)^2}\frac{Z_0 Z_s}{Z^2}\frac{1}{\left(\sin \phi_s\right)^2}\frac{l_s}{v_p} \tag{11}$$

v_p being the phase velocity of the sensing line. Evaluation of (11) at the resonance frequency (the operational frequency), where ϕ_s = 90º gives:

$$\left.\frac{d\phi_\rho}{d\omega}\right|_{\omega_0} = -\frac{2Z_0 Z_s}{Z^2}\frac{l_s}{v_p} \tag{12}$$

and it is apparent that the magnitude of the phase slope increases by increasing Z_s and by decreasing Z. Note that the first term in the right-hand side member of (12) (involving the line impedances) exhibits the same dependence than the sensitivity in the limit of small perturbations, given by (5). Thus, it is clear, according to (12), that sensitivity enhancement requires a high phase slope (achieved through impedance contrast between the design line and the sensing line), an aspect not discussed in [60].

Another interesting aspect concerns the analogy between the considered 90º open-ended sensing line (resonator) and a series resonator. Indeed, both structures exhibit a similar behavior in the vicinity of resonance, provided the reactive elements of the resonator are properly mapped to the characteristic impedance of the sensing line. Let us next discuss this aspect by calculating the phase slope at resonance of the structure of Fig. 1 but replacing the 90º open-ended line with a series LC resonator. In this case, the impedance of the resonator is simply:

$$Z_{\text{in,s}} = j\left(L\omega - \frac{1}{C\omega}\right) \tag{13}$$

and the reflection coefficient is

$$\rho = \frac{\frac{Z^2}{Z_0} - j\left(L\omega - \frac{1}{C\omega}\right)}{\frac{Z^2}{Z_0} + j\left(L\omega - \frac{1}{C\omega}\right)} \tag{14}$$

The phase of the reflection coefficient is thus:

$$\phi_\rho = 2\arctan\left\{-\frac{Z_0}{Z^2}\left(L\omega - \frac{1}{C\omega}\right)\right\} \tag{15}$$

Deriving with the angular frequency gives:

$$\frac{d\phi_\rho}{d\omega} = -\frac{2}{1+\left\{\frac{Z_0}{Z^2}\left(L\omega - \frac{1}{C\omega}\right)\right\}^2}\cdot\frac{Z_0}{Z^2}\left(L + \frac{1}{C\omega^2}\right) \tag{16}$$

and evaluation at resonance provides:

$$\left.\frac{d\phi_\rho}{d\omega}\right|_{\omega_0 = 1/\sqrt{LC}} = -4L\frac{Z_0}{Z^2} \tag{17}$$

Note that (12) and (17) are identical provided:

$$Z_s\frac{l_s}{v_p} = 2L \tag{18}$$

or

$$Z_s\omega_0\frac{l_s}{v_p} = 2\omega_0 L \tag{19}$$

Since at resonance the electrical length of the line is 90º, the previous expression can be written as

$$Z_s\frac{\pi}{2} = 2\omega_0 L \tag{20}$$

and, finally,

$$Z_s = \frac{4}{\pi}\sqrt{\frac{L}{C}} \tag{21}$$

which is the above-cited mapping, necessary to obtain an identical behavior between both sensing elements, the 90º open-ended sensing line and the series LC sensing resonator.

Based on the previous equivalence, let us next analyze the effects of LUT losses (this is justified since liquids, especially mixtures of DI water and ethanol, are lossy samples [71]-[73]). Considering losses in the equivalent series LC resonator of the 90º open-ended sensing line is as simple as including a series resistance, *R*, in the model. Thus, the reflection coefficient (14) should be expressed as

$$\rho = \frac{\frac{Z^2}{Z_0} - R - j\left(L\omega - \frac{1}{C\omega}\right)}{\frac{Z^2}{Z_0} + R + j\left(L\omega - \frac{1}{C\omega}\right)} \tag{22}$$

and the phase of the reflection coefficient is thus

$$\phi_\rho = \arctan\left\{-\frac{L\omega-\frac{1}{C\omega}}{\frac{Z^2}{Z_0}-R}\right\} - \arctan\left\{\frac{L\omega-\frac{1}{C\omega}}{\frac{Z^2}{Z_0}+R}\right\} \quad (23)$$

The derivative of the phase of the reflection coefficient with the angular frequency evaluated at the resonance frequency is found to be

$$\left.\frac{d\phi_\rho}{d\omega}\right|_{\omega_0=1/\sqrt{LC}} = -4L\frac{Z_0}{Z^2}\cdot\frac{1}{1-R^2\frac{Z_0^2}{Z^4}} \quad (24)$$

which means that losses might help to boost up the magnitude of the phase slope, and consequently the sensitivity in the limit of small perturbations. Typically, the term $R^2Z_0^2/Z^4 < 1$, and the sign of the phase slope (negative) is preserved (this can be appreciated in Fig. 5). Expression (24) provides a qualitative explanation of the slight discrepancy between the theoretical sensitivity (–1.09º), calculated previously by excluding the effects of losses, and the one inferred by simulation (–1.16º) or experimentally (–1.18º), where losses are included and boost up the sensitivity.

Let us next try to link L and R in (24) with the electrical elements describing the sensing line, i.e., Z_s and the attenuation constant, α. Concerning L, expression (18) provides such link. Regarding R, let us first express the impedance of the open-ended sensing line by including losses. Such impedance is [70]

$$Z_{in,s} = Z_s \coth \gamma l_s \quad (25)$$

where $\gamma = \alpha + j\beta$ is the complex propagation constant of the sensing line (β is the phase constant, so that $\phi_s = \beta l_s$). Expression (25) can be rewritten as

$$Z_{in,s} = Z_s\frac{\sinh 2\alpha l_s - j\sin 2\phi_s}{\cosh 2\alpha l_s - \cos 2\phi_s} \quad (26)$$

and it is apparent that at resonance (where ϕ_s = 90º), the impedance $Z_{in,s}$, purely resistive and identifiable with R, is

$$Z_{in,s}\big|_{\phi_s=\pi/2} = Z_s\frac{\sinh 2\alpha l_s}{\cosh 2\alpha l_s + 1} = Z_s\frac{\sinh \alpha l_s}{\cosh \alpha l_s} = R \quad (27)$$

Hence, (24) can be rewritten as

$$\left.\frac{d\phi_\rho}{d\omega}\right|_{\omega_0=1/\sqrt{LC}} = -2\left(Z_s\frac{l_s}{v_p}\right)\frac{Z_0}{Z^2}\cdot\frac{1}{1-(\tanh\alpha l_s)^2\frac{Z_s^2Z_0^2}{Z^4}} \quad (28)$$

It is obvious that if we exclude the term l_s/v_p in (28), the resulting derivative is $d\phi_\rho/d\phi_s\big|_{\phi_s=\pi/2}$. Therefore, the sensitivity (5) by including the effects of losses is

$$S = -\frac{Z_sZ_0}{Z^2}\cdot\frac{1}{1-(\tanh\alpha l_s)^2\frac{Z_s^2Z_0^2}{Z^4}}\frac{\phi_s}{\varepsilon_{\text{eff}}}\frac{d\varepsilon_{\text{eff}}}{d\varepsilon_{\text{LUT}}} \quad (29)$$

since

$$\frac{d\phi_s}{d\varepsilon_{\text{eff}}} = \frac{d}{d\varepsilon_{\text{eff}}}\left(\frac{\omega}{c}l_s\sqrt{\varepsilon_{\text{eff}}}\right) = \frac{\phi_s}{2\varepsilon_{\text{eff}}} \quad (30)$$

c being the speed of light in vacuum. Note that if losses are absent, (29) coincides with (5), as expected.

Estimation of the attenuation constant, or, more specifically, αl_s, can be done from electromagnetic simulation of the sensing line (i.e., by excluding the design line) coated with the REF liquid (pure DI water). At resonance, where the input impedance $Z_{in,s}$ is purely real and given by R, the reflection coefficient is located in the horizontal axis in the Smith chart, from where we can infer the value of R. Then, using (27), αl_s can be retrieved. The value that has been obtained is αl_s = 0.023 Np. Introducing this value in (29), the theoretical sensitivity in the limit of small perturbations by including losses is found to be S_{th} = –1.11, closer to the experimental value given in Fig. 6. Nevertheless, the accurate determination of the sensitivity from the measured data is complicated, and this explains that, even by including the effects of losses in the analysis, the theoretical prediction slightly deviates from the measured sensitivity.

VI. Conclusions

In conclusion, a novel one-port reflective-mode phase-variation submersible sensor based on planar technology has been presented. The sensor is comprised of a step-impedance microstrip line configuration, i.e., a sensing line (an open-ended quarter-wavelength microstrip line with high impedance) cascaded to a design line (a quarter-wavelength microstrip line with low impedance). This constitutes the microwave module. Moreover, in order to protect the non-sensitive region of the sensor against liquid leakage, a 3D-printed case (mechanical module) has been fabricated and assembled to the sensor substrate. The output variable of the sensor (the phase of the reflection coefficient) exhibits moderately good sensitivity with the dielectric constant of the LUT, mixtures of ethanol and DI water in this paper, and very good linearity in the input dynamic range. The achieved resolution is 2%. As compared to other submersible sensors, where the output variable is the notch frequency in either the reflection or transmission coefficient, the proposed device works at a single frequency. Moreover, the achieved sensitivity with the concentration of ethanol in DI water (1.22º/%) and resolution can be boosted up, if necessary, by simply adding extra quarter-wavelength design lines with alternating high/low characteristic impedance.

References

[1] F. Martín, P. Vélez, J. Muñoz-Enano and L.Su, *Planar Microwave Sensors*, Wiley/IEEE Press, Hoboken, NJ, USA, 2022.

[2] J. Yeo, J. I. Lee, and Y. Kwon, "Humidity-sensing chipless RFID tag with enhanced sensitivity using an interdigital capacitor structure," Sensors, vol. 21, paper 6550, 2021.

[3] E. M. Amin, M. S. Bhuiyan, N. C. Karmakar, and B. Winther-Jensen, "Development of a low cost printable chipless RFID humidity sensor," IEEE Sensors J., vol. 14, no. 1, pp. 140–149, Jan. 2014.

[4] D. Girbau, Á. Ramos, A. Lazaro, S. Rima, and R. Villarino, "Passive wireless temperature sensor based on time-coded UWB chipless RFID tags," *IEEE Trans. Microw. Theory Techn.*, vol. 60, no. 11, pp. 3623–3632, Nov. 2012.

[5] W. M. Abdulkawi and A. F. A. Sheta, "Chipless RFID sensors based on multistate coupled line resonators," *Sens. Act. A: Phys.*, vol. 309, paper 112025, Jul. 2020.

[6] J. Naqui and F. Martín, "Transmission lines loaded with bisymmetric resonators and their application to angular displacement and velocity

sensors," *IEEE Trans. Microw. Theory Techn*., vol. 61, no. 12, pp. 4700–4713, Dec. 2013.

[7] A.K. Horestani, J. Naqui, D. Abbott, C. Fumeaux, and F. Martín, "Two-dimensional displacement and alignment sensor based on reflection coefficients of open microstrip lines loaded with split ring resonators," *Elec. Lett.*, vol. 50, pp. 620–622, Apr. 2014.

[8] A. Ebrahimi, W. Withayachumnankul, S. F. Al-Sarawi, and D. Abbott, "Metamaterial-inspired rotation sensor with wide dynamic range," *IEEE Sens. J*., vol. 14, no. 8, pp. 2609-2614, Aug. 2014.

[9] J. Mata-Contreras, C. Herrojo, and F. Martín, "Application of split ring resonator (SRR) loaded transmission lines to the design of angular displacement and velocity sensors for space applications," *IEEE Trans. Microw. Theory Techn*., vol. 65, pp. 4450–4460, Nov. 2017.

[10] F. Paredes, C. Herrojo, A. Moya, M. Berenguel-Alonso, D. Gonzalez, J. Bruguera, C. Delgado-Simao, and F. Martín, "Electromagnetic encoders screen-printed on rubber belts for absolute measurement of position and velocity," *Sensors*, vol. 22, paper 2044, 2022.

[11] C. Occhiuzzi, A. Rida, G. Marrocco, and M. Tentzeris, "RFID passive gas sensor integrating carbon nanotubes," *IEEE Trans. Microw. Theory Techn.*, vol. 59, no. 10, pp. 2674–2684, Oct. 2011.

[12] R. A. Potyrailo and C. Surman, "A passive radio-frequency identification (RFID) gas sensor with self-correction against fluctuations of ambient temperature," *Sens. Act. B: Chem.*, vol 185, pp. 587–593, 2013.

[13] R. Narang, S. Mohammadi, M.M. Ashani, H. Sadabadi, H. Hejazi, M.H. Zarifi, and A. Sanati-Nezhad, "Sensitive, real-time and non-intrusive detection of concentration and growth of pathogenic bacteria using microfluidic-microwave ring resonator biosensor," *Sci. Rep.*, vol. 8, no. 1, paper 15807, 2018.

[14] J. Muñoz-Enano, P. Vélez, M. Gil, E. Jose-Cunilleras, A. Bassols, and F. Martín, "Characterization of electrolyte content in urine samples through a differential microfluidic sensor based on dumbbell-shaped defect ground structures", *Int. J. Microwaves Wireless Technol*., vol. 12, no. 9, pp. 817–824, 2020.

[15] M.C. Jain, A.V. Nadaraja, R. Narang, and M.H. Zarifi, "Rapid and real-time monitoring of bacterial growth against antibiotics in solid growth medium using a contactless planar microwave resonator sensor," *Sci. Rep.*,vol. 11, no. 1, paper 14775, 2021.

[16] M. Gil, P. Vélez, F. Aznar, J. Muñoz-Enano, and F. Martín, "Differential sensor based on electro-inductive wave (EIW) transmission lines for dielectric constant measurements and defect detection," *IEEE Trans. Ant. Propag*., vol. 68, pp. 1876–1886, Mar. 2020.

[17] C. Herrojo, P. Vélez, J. Muñoz-Enano, L. Su, P. Casacuberta, M. Gil, and F. Martín, "Highly sensitive defect detectors and comparators exploiting port imbalance in rat-race couplers loaded with step-impedance open-ended transmission lines," *IEEE Sensors J*., vol. 21, no. 23, pp. 26731–26745, Dec. 2021.

[18] B. Ebrahimi, W. Withayachumnankul, S. Al-Sarawi, and D. Abbott, "High-sensitivity metamaterial-inspired sensor for microfluidic dielectric characterization," *IEEE Sensors J.*, vol. 14, no. 5, pp. 1345−1351, May 2014.

[19] P. Vélez, K. Grenier, J. Mata-Contreras, D. Dubuc, and F. Martín, "Highly-sensitive microwave sensors based on open complementary split ring resonators (OCSRRs) for dielectric characterization and solute concentration measurements in liquids," *IEEE Access*, vol. 6, pp. 48324–48338, Dec. 2018.

[20] P. Vélez, J. Muñoz-Enano, K. Grenier, J. Mata-Contreras, D. Dubuc, and F. Martín, "Split ring resonator (SRR) based microwave fluidic sensor for electrolyte concentration measurements," *IEEE Sensors J*., vol. 19, no. 7, pp. 2562–2569, Apr. 2019.

[21] N. Hosseini, M. Baghelani, and M. Daneshmand, "Selective volume fraction sensing using resonant-based microwave sensor and its harmonics," *IEEE Trans. Microw. Theory Techn.*, vol. 68, no. 9, pp. 3958–3968, Sep. 2020.

[22] N. Hosseini and M. Baghelani, "Selective real-time non-contact multi-variable water-alcohol-sugar concentration analysis during fermentation process using microwave split-ring resonator based sensor," *Sens. Act. A: Phys.*, vol. 325, pp, 112695, 2021.

[23] P. Vélez, L. Su, K. Grenier, J. Mata-Contreras, D. Dubuc, and F. Martín, "Microwave microfluidic sensor based on a microstrip splitter/combiner configuration and split ring resonators (SRR) for dielectric characterization of liquids," *IEEE Sens. J*., vol. 17, pp. 6589–6598, Oct. 2017.

[24] M.H. Zarifi, H. Sadabadi, S.H. Hejazi, M. Daneshmand, and A. Sanati-Nezhad "Noncontact and nonintrusive microwave-microfluidic flow sensor for energy and biomedical engineering," *Sci. Rep.*, vol. 8, paper 139, 2018.

[25] A. Ebrahimi, J. Scott, and K. Ghorbani, "Ultrahigh-sensitivity microwave sensor for microfluidic complex permittivity measurement," *IEEE Trans. Microw. Theory Techn.*, vol. 67, no. 10, pp. 4269–4277, Oct. 2019.

[26] A. Ebrahimi, F.J. Tovar-Lopez, J. Scott, and K. Ghorbani, "Differential microwave sensor for characterization of glycerol–water solutions," *Sensors and Actuators B: Chemical*, vol. 321, paper 128561, 2020.

[27] L. Su, J. Mata-Contreras, P. Vélez, A. Fernández-Prieto, and F. Martín, "Analytical method to estimate the complex permittivity of oil samples," *Sensors*, vol. 18, paper 984, 2018.

[28] J. Muñoz-Enano, P. Vélez, M. Gil, and F. Martín, "Frequency variation sensors for permittivity measurements based on dumbbell-shaped defect ground structures (DB-DGS): analytical method and sensitivity analysis," *IEEE Sensors J.*, vol. 22, no. 10, pp. 9378–9386, May 2022.

[29] M. A. Stuchly and S. S. Stuchly, "Coaxial line reflection methods for measuring dielectric properties of biological substances at radio and microwave frequencies—A review," *IEEE Trans. Instrum. Meas*., vol. 29, pp. 176–183, 1980.

[30] E. Burdette, F. Cain, and J. Seals, "In vivo probe measurement technique for determining dielectric properties at VHF through microwave frequencies," *IEEE Trans. Microw. Theory Techn*., vol. 28, pp. 414–427, 1980.

[31] T.W. Athey, M.A. Stuchly, and S.S. Stuchly, "Measurement of radio frequency permittivity of biological tissues with an open-ended coaxial line: Part 1," *IEEE Trans. Microw Theory Techn*., vol. 30, no. 1, pp. 82–86, Jan. 1982.

[32] S. Gabriel, R.W. Lau, and C. Gabriel, "The dielectric properties of biological tissues: II. measurements in the frequency range 10 Hz to 20 GHz," *Phys. Med. Biol*., vol. 41, pp. 2251–2269, 1996.

[33] S.A. Komarov, A.S. Komarov, D.G. Barber, M.J.L. Lemes, and S. Rysgaard, "Open-ended coaxial probe technique for dielectric spectroscopy of artificially grown sea ice," *IEEE Transactions on Geoscience and Remote Sensing*, vol. 54, no. 8, pp. 4941–4951, Aug. 2016.

[34] A. La Gioia, E. Porter, I. Merunka, A. Shahzad, S. Salahuddin, M. Jones, and M. O'Halloran, "Open-ended coaxial probe technique for dielectric measurement of biological tissues: challenges and common practices," *Diagnostics*, vol. 8, paper 40, 2018.

[35] C. Aydinalp, S. Joof, and T. Yilmaz, "Towards non-invasive diagnosis of skin cancer: sensing depth investigation of open-ended coaxial probes," *Sensors*, vol. 21, paper 1319, 2021.

[36] Keysight Technologies, N1501A Dielectric Probe Kit:10 MHz to 50 GHz, Technical Overview, 2020.

[37] G. Galindo-Romera, F.J. Herraiz-Martínez, M. Gil, J.J. Martínez-Martínez and D. Segovia-Vargas, "Submersible printed split-ring resonator-based sensor for thin-film detection and permittivity characterization," *IEEE Sensors J.*, vol. 16, no. 10, pp. 3587–3596, May 2016.

[38] E. Reyes-Vera, G. Acevedo-Osorio, Mauricio Arias-Correa, and David E. Senior, "A submersible printed sensor based on a monopole-coupled split ring resonator for permittivity characterization," *Sensors*, vol. 19, no. 8, paper 1936, 2019.

[39] A. Nuñez-Flores, P. Castillo-Araníbar, A. García-Lampérez, and D. Segovia-Vargas, "Design and implementation of a submersible split ring resonator based sensor for pisco concentration measurements," *2018 IEEE MTT-S Latin America Microwave Conference* (LAMC 2018), Arequipa, Peru, Dec. 2018.

[40] X. Zhang, C. Ruan, W. Wang, and Y. Cao, "Submersible high sensitivity microwave sensor for edible oil detection and quality analysis," *IEEE Sensors J*., vol. 21, no. 12, pp. 13230–13238, Jun. 2021.

[41] M. Puentes, C. Weiß, M. Schüßler, and R. Jakoby, "Sensor array based on split ring resonators for analysis of organic tissues," *IEEE MTT-S Int. Microw. Symp.*, Baltimore, MD, USA, Jun. 2011, pp. 1−4.

[42] M.S. Boybay and O.M. Ramahi, "Material characterization using complementary split-ring resonators," *IEEE Trans. Instrum. Meas.*, vol. 61, no. 11, pp. 3039−3046, Nov. 2012.

[43] C.S. Lee and C.L. Yang, "Complementary split-ring resonators for measuring dielectric constants and loss tangents," *IEEE Microw. Wireless Compon. Lett.*, vol. 24, no. 8, pp. 563−565, Aug. 2014.

[44] C.L. Yang, C.S. Lee, K.W. Chen, and K.Z. Chen, "Noncontact measurement of complex permittivity and thickness by using planar resonators," *IEEE Trans. Microw. Theory Techn.*, vol. 64, no.1, pp. 247−257, Jan. 2016.

[45] M. Abdolrazzaghi, M.H. Zarifi, and M. Daneshmand, "Sensitivity enhancement of split ring resonator based liquid sensors," *2016 IEEE Sensors*, 2016, pp. 1−3, doi: 10.1109/ICSENS.2016.7808957.
[46] M. Abdolrazzaghi, M. Daneshmand, and A.K. Iyer, "Strongly enhanced sensitivity in planar microwave sensors based on metamaterial coupling," *IEEE Trans. Microw. Theory Techn*., vol. 66, no. 4, pp. 1843−1855, Apr. 2018.
[47] A.K. Jha, N. Delmonte, A. Lamecki, M. Mrozowski, and M. Bozzi, "Design of microwave-based angular displacement sensor," *IEEE Microw. Wireless Compon. Lett.*, vol. 29, no. 4, pp. 306−308, Apr. 2019.
[48] M. Abdolrazzaghi and M. Daneshmand, "Exploiting sensitivity enhancement in micro-wave planar sensors using intermodulation products with phase noise analysis," *IEEE Trans. Circ. Syst. I: Reg. Pap.*, vol. 67, no. 12, pp. 4382–4395, Dec. 2020.
[49] A.M. Albishi, M.K.E. Badawe, V. Nayyeri, and O.M. Ramahi, "Enhancing the sensitivity of dielectric sensors with multiple coupled complementary split-ring resonators," *IEEE Trans. Microw. Theory Techn.*, vol. 68, no. 10, pp. 4340–4347, Oct. 2020.
[50] A. Aquino, C.G. Juan, B. Potelon, and C. Quendo, "Dielectric permittivity sensor based on planar open-loop resonator," *IEEE Sensors Lett*., vol. 5, no. 3, pp. 1–4, Mar. 2021, Art no. 3500204.
[51] J. Naqui, M. Durán-Sindreu, and F. Martín, "Novel sensors based on the symmetry properties of split ring resonators (SRRs)," *Sensors*, vol 11, pp. 7545−7553, 2011.
[52] A.K. Horestani, C. Fumeaux, S.F. Al-Sarawi, and D. Abbott, "Displacement sensor based on diamond-shaped tapered split ring resonator," *IEEE Sens. J*., vol. 13, pp. 1153–1160, 2013.
[53] A.K. Horestani, D. Abbott, and C. Fumeaux, "Rotation sensor based on horn-shaped split ring resonator," *IEEE Sens. J.*, vol. 13, pp. 3014–3015, 2013.
[54] J. Naqui and F. Martín, "Angular displacement and velocity sensors based on electric-LC (ELC) loaded microstrip lines," *IEEE Sens. J.*, vol. 14, no. 4, pp. 939–940, Apr. 2014.
[55] A. Ebrahimi, W. Withayachumnankul, S.F. Al-Sarawi, and D. Abbott, "Metamaterial-inspired rotation sensor with wide dynamic range," *IEEE Sens. J*., vol. 14, no. 8, pp. 2609–2614, Aug. 2014.
[56] J. Mata-Contreras, C. Herrojo, and F. Martín, "Detecting the rotation direction in contactless angular velocity sensors implemented with rotors loaded with multiple chains of split ring resonators (SRRs)," *IEEE Sens. J*., vol.18, no. 17, pp. 7055–7065, Sep. 2018.
[57] F.J. Ferrández-Pastor, J.M. García-Chamizo, and M. Nieto-Hidalgo, "Electromagnetic differential measuring method: application in microstrip sensors developing," *Sensors*, vol. 17, paper 1650, 2017.
[58] J. Muñoz-Enano, P. Vélez, M. Gil, and F. Martín, "An analytical method to implement high sensitivity transmission line differential sensors for dielectric constant measurements," *IEEE Sensors J*., vol. 20, pp. 178–184, Jan. 2020.
[59] A. Ebrahimi, J. Coromina, J. Muñoz-Enano, P. Vélez, J. Scott, K. Ghorbani, and F. Martín, "Highly sensitive phase-variation dielectric constant sensor based on a capacitively-loaded slow-wave transmission line," *IEEE Trans. Circ. Syst. I: Reg. Pap*., vol. 68, no. 7, pp. 2787–2799, Jul. 2021.
[60] J. Muñoz-Enano, P. Vélez, L. Su, M. Gil, P. Casacuberta, and F. Martín, "On the sensitivity of reflective-mode phase variation sensors based on open-ended stepped-impedance transmission lines: theoretical analysis and experimental validation," *IEEE Trans. Microw. Theory Techn*. vol. 69, no. 1, pp. 308–324, Jan. 2021.
[61] L. Su, J. Muñoz-Enano, P. Vélez, P. Casacuberta, M. Gil, and F. Martín "Highly sensitive phase variation sensors based on step-impedance coplanar waveguide (CPW) transmission lines for dielectric characterization," *IEEE Sensors J*., vol. 21, no. 3, pp. 2864–2872, Feb. 2021.
[62] P. Casacuberta, J. Muñoz-Enano, P. Vélez, L. Su, M. Gil, and F. Martín, "Highly sensitive reflective-mode detectors and dielectric constant sensors based on open-ended stepped-impedance transmission lines," *Sensors*, vol. 20, paper 6236, 2020.
[63] A.K. Jha, A. Lamecki, M. Mrozowski, and M. Bozzi, "A highly sensitive planar microwave sensor for detecting direction and angle of rotation," *IEEE Trans. Microw. Theory Techn*., vol. 68, no. 4, pp. 1598–1609, Apr. 2020.
[64] A.K. Horestani, Z. Shaterian, and F. Martín, "Rotation sensor based on the cross-polarized excitation of split ring resonators (SRRs)," *IEEE Sensors J*., vol 20, pp. 9706–9714, Sep. 2020.
[65] J. Muñoz-Enano, P. Vélez, L. Su, M. Gil, and F. Martín, "A reflective-mode phase-variation displacement sensor," *IEEE Access*, vol. 8, pp. 189565–189575, Oct. 2020.
[66] L. Su, J. Muñoz-Enano, P. Vélez, P. Casacuberta, M. Gil, and F. Martín, "Phase-variation microwave sensor for permittivity measurements based on a high-impedance half-wavelength transmission line," *IEEE Sensors J*., vol. 21, no. 9, pp. 10647–10656, May 2021.
[67] L. Su, J Muñoz-Enano, P. Vélez, M. Gil, P. Casacuberta, and F. Martín, "Highly sensitive reflective-mode phase-variation permittivity sensor based on a coplanar waveguide (CPW) terminated with an open complementary split ring resonator (OCSRR)," *IEEE Access*, vol. 9, pp. 27928–27944, 2021.
[68] P. Casacuberta, J. Muñoz-Enano, P. Vélez, L. Su, M. Gil, A. Ebrahimi, and F. Martín, "Circuit analysis of a Coplanar waveguide (CPW) terminated with a step-impedance resonator (SIR) for highly sensitive one-port permittivity sensing," *IEEE Access*, vol. 10, pp. 62597–62612, 2022.
[69] O. Weiner, "Die theorie des Mischkorpers fur das feld der statonare Stromung i. Die mittelwertsatze fur kraft, polarisation und energie," *Trans. Math.-Phys. Class Roy. Saxon Soc. Sci*., vol. 32, pp. 509–604,1912.
[70] D.M. Pozar, *Microwave Engineering*, 4th Ed., John Wiley, Hoboken, NJ, USA, 2012.
[71] T. Karpisz, P. Kopyt, B. Salski, and J. Krupka, "Open-ended waveguide measurement of liquids at millimeter wavelengths," *2016 IEEE MTT-S International Microwave Symposium* (IMS), San Francisco, CA, USA, 22–27 May 2016.
[72] J. Krupka, "Measurements of the complex permittivity of highly concentrated aqueous NaCl solutions and ferrofluid employing microwave cylindrical cavities," *Measurement Science and Technology*, vol. 26, no. 9, p. 095702, Jul. 2015.
[73] A. Stefanski, and J. Krupka, "Complex permittivity measurements of lossy liquids at microwave frequencies," *MIKON 2008-17th International Conference on Microwaves, Radar and Wireless Communications*, Wroclaw, Poland, 19–21 May 2008.

Lijuan Su (Member, IEEE) was born in Qianjiang (Hubei), China in 1983. She received the B.S. degree in communication engineering and the M.S. degree in circuits and systems both from Wuhan University of Technology, Wuhan, China, in 2005 and 2013 respectively, and the Ph.D. degree in electronic engineering from Universitat Autonoma de Barcelona, Barcelona, Spain, in 2017. From Nov. 2017 to Dec. 2019, she worked as a postdoc researcher in Flexible Electronics Research Center, Huazhong University of Science and Technology, Wuhan, China. She is currently a postdoc researcher in CIMITEC, Universitat Autonoma de Barcelona, Spain. Her current research interests focus on the development of novel microwave sensors with improved performance for biosensors, dielectric characterization of solids and liquids, defect detection, industrial processes, etc.

Paris Vélez (Senior Member, IEEE) was born in Barcelona, Spain, in 1982. He received the degree in Telecommunications Engineering, specializing in electronics, the Electronics Engineering degree, and the Ph.D. degree in Electrical Engineering from the Universitat Autònoma de Barcelona, Barcelona, in 2008, 2010, and 2014, respectively. His Ph.D. thesis concerned common mode suppression differential microwave circuits based on metamaterial concepts and semi-lumped resonators. During the Ph.D., he was awarded with a pre-doctoral teaching and research fellowship by the Spanish Government from 2011 to 2014. From 2015-2017, he was involved in the subjects related to metamaterials sensors for fluidics detection and characterization at LAAS-CNRS through a TECNIOSpring fellowship cofounded by the Marie Curie program. His current research interests include the miniaturization of passive circuits RF/microwave and sensors-based metamaterials through Juan de la Cierva fellowship. Dr. Vélez is a Reviewer for the IEEE Transactions on Microwave Theory and Techniques and for other journals.

Pau Casacuberta (Graduate Student Member, IEEE) was born in Sabadell (Barcelona), Spain, in 1997. Currently he is in his senior year of the Bachelor's degree in Electronic Telecommunications Engineering and the Bachelor's Degree in Computer Engineering, both at the Universitat Autònoma de Barcelona (UAB). He received the Collaboration fellowship by the Spanish Government in 2019 and developing his Bachelor's Thesis in highly sensitive microwave sensors based in stepped impedance structures.

Jonathan Muñoz-Enano (Member, IEEE) was born in Mollet del Vallès (Barcelona), Spain, in 1994. He received the Bachelor's degree in Electronic Telecommunications Engineering in 2016 and the Master's Degree in Telecommunications Engineering in 2018, both at the Autonomous University of Barcelona (UAB). In July 2022, he obtained the PhD degree within the doctoral program in Electronics Engineering and Telecommunications in the same university. Currently he is working as a postdoctoral researcher in CIMITEC, Universitat Autònoma de Barcelona, Spain. His current research interests focus on the development of microwave sensors based on metamaterial concepts for the dielectric characterization of materials and biosensors.

Marta Gil-Barba (Member, IEEE) was born in Valdepeñas, Ciudad Real, Spain, in 1981. She received the Physics degree from Universidad de Granada, Spain, in 2005, and the Ph.D. degree in electronic engineering from the Universitat Autònoma de Barcelona, Barcelona, Spain, in 2009. She studied one year with the Friedrich Schiller Universität Jena, Jena, Germany. During her PhD Thesis she was holder of a METAMORPHOSE NoE grant and National Research Fellowship from the FPU Program of the Education and Science Spanish Ministry. As a postdoctoral researcher, she was awarded with a Juan de la Cierva fellowship working in the Universidad de Castilla-La Mancha. She was postdoctoral researcher in the Institut für Mikrowellentechnik und Photonik in Technische Universität Darmstadt and in the Carlos III University of Madrid. She is currently assistant professor in the Universidad Politécnica de Madrid. She has worked in metamaterials, piezoelectric MEMS and microwave passive devices. Her current interests include metamaterials sensors for fluidic detection.

Ferran Martín (Fellow, IEEE) was born in Barakaldo (Vizcaya), Spain in 1965. He received the B.S. Degree in Physics from the Universitat Autònoma de Barcelona (UAB) in 1988 and the PhD degree in 1992. From 1994 up to 2006 he was Associate Professor in Electronics at the Departament d'Enginyeria Electrònica (Universitat Autònoma de Barcelona), and since 2007 he is Full Professor of Electronics. In recent years, he has been involved in different research activities including modelling and simulation of electron devices for high frequency applications, millimeter wave and THz generation systems, and the application of electromagnetic bandgaps to microwave and millimeter wave circuits. He is now very active in the field of metamaterials and their application to the miniaturization and optimization of microwave circuits and antennas. Other topics of interest include microwave sensors and RFID systems, with special emphasis on the development of high data capacity chipless-RFID tags. He is the head of the Microwave Engineering, Metamaterials and Antennas Group (GEMMA Group) at UAB, and director of CIMITEC, a research Center on Metamaterials supported by TECNIO (Generalitat de Catalunya). He has organized several international events related to metamaterials and related topics, including Workshops at the IEEE International Microwave Symposium (years 2005 and 2007) and European Microwave Conference (2009, 2015 and 2017), and the Fifth International Congress on Advanced Electromagnetic Materials in Microwaves and Optics (Metamaterials 2011), where he acted as Chair of the Local Organizing Committee. He has acted as Guest Editor for six Special Issues on metamaterials and sensors in five International Journals. He has authored and co-authored over 650 technical conference, letter, journal papers and book chapters, he is co-author of the book on Metamaterials entitled *Metamaterials with Negative Parameters: Theory, Design and Microwave Applications* (John Wiley & Sons Inc.), author of the book *Artificial Transmission Lines for RF and Microwave Applications* (John Wiley & Sons Inc.), co-editor of the book *Balanced Microwave Filters* (Wiley/IEEE Press), co-author of the book *Time-Domain Signature Barcodes for Chipless-RFID and Sensing Applications* (Springer), and co-author of the book *Planar Microwave Sensors* (Wiley/IEEE Press). Ferran Martín has generated 22 PhDs, has filed several patents on metamaterials and has headed several Development Contracts.

Prof. Martín is a member of the IEEE Microwave Theory and Techniques Society (IEEE MTT-S). He is reviewer of the IEEE Transactions on Microwave Theory and Techniques and IEEE Microwave and Wireless Components Letters, among many other journals, and he serves as member of the Editorial Board of IET Microwaves, Antennas and Propagation, International Journal of RF and Microwave Computer-Aided Engineering, and Sensors. He is also a member of the Technical Committees of the European Microwave Conference (EuMC) and International Congress on Advanced Electromagnetic Materials in Microwaves and Optics (Metamaterials). Among his distinctions, Ferran Martín has received the 2006 Duran Farell Prize for Technological Research, he holds the *Parc de Recerca UAB – Santander* Technology Transfer Chair, and he has been the recipient of three ICREA ACADEMIA Awards (calls 2008, 2013 and 2018). He is Fellow of the IEEE and Fellow of the IET.